Calibration and Allan Variance Analyses of Inertial Measurement Unit

[1]Ritesh Parmar, [2]Dinesh Yadav, [3]Vipan Kumar
[1]Student, [2]Assistant Professor, [3]Senior Scientist
[1, 2]Department of Electronics and Communication Engineering
[3]Department of Optical Devices and Systems
[1, 2]Manipal University Jaipur, Jaipur, India- 303007
[3]CSIR-Central Scientific Instruments Organisation, Chandigarh, India-160030

***Abstract* - Inertial measurement unit consists of gyroscopes and accelerometers, which are known as inertial sensors. These sensors are prone to various deterministic and random errors which need to be compensated. This work presents a calibration and stochastic modeling technique for six degree of freedom inertial measurement unit in order to remove these errors from inertial sensors. Calibration of inertial measurement unit is carried out to estimate the coefficients which transform the raw output of sensors into meaningful data. In this paper, allan variance technique is used to model and analyze various random errors present in inertial sensors. This paper covers the theoretical basis of calibration and allan variance along with implementation of these techniques to inertial sensors.**

***Index Terms* - Inertial measurement unit, calibration, deterministic errors, allan variance, inertial sensors, random errors**

I. INTRODUCTION

In aerospace systems, universal problem is that of determining the attitude of spacecraft with respect to selected reference frame. A common way to determine attitude is to fuse together the data from gyroscopes, accelerometers and other attitude sensors [1]. Inertial navigation system provides accurate attitude estimate for short time intervals but suffers from accuracy degradation with time due to combined effects of errors present in inertial sensors [2]. The requirement for accurate estimation of aircraft attitude necessitates the calibration and stochastic error modeling of inertial sensors.

Errors which exist in inertial sensors can be divided into two parts: random and deterministic errors [3]. In deterministic errors there is some relationship between the input and output of the sensor whereas in random errors there in no such kind of empirical relationship between them. Deterministic errors are due to manufacturing defects and can be calibrated out from the data [4]. Deterministic errors include bias, scale factor and non-orthogonality. Ideally, when no input is applied to the sensor, the output from the sensor should read zero. But, this is not the case and the offset is called bias of sensor [5]. Scale factor is the change in output to a change in the intended input to be measured. It is calculated as the slope of straight line that can be fitted to the input -output data. An ideal sensor has a scale factor of one [6]. Weak signal detection and extraction from sensor can introduce the scale factor error. Non-orthogonality errors arise when the axes of sensor triad are not perfectly orthogonal (at right angle) [7]. Noise is an additional signal resulting from the sensor itself or other electronic equipment that interferes with the output signals trying to measure. Noise is in general non- systematic and therefore cannot be removed from the data using deterministic models [2]. It can only be modeled by stochastic process.

In this paper, we aim to establish a calibration and allan variance method for the identification of various deterministic as well as random error coefficients.

II. CALIBRATION

Calibration is the process of comparing instrument output with known reference information and determining the coefficients that force the output to agree with the reference information over a range of output values [2]. To determine the bias, scale factor and non-orthogonal error parameters, the first step in inertial navigation is to calibrate its sensors.

In this calibration procedure, the Earth's gravity is used as the physical standard for calibrating the IMU; it is freely available and is a very steady quantity [8] and misalignment matrix as represented in [9] is used for the generation of calibration model for accelerometer and gyroscope. A tri-axial accelerometer is calibrated using property (p1): the magnitude of the static acceleration measured must equal that of the gravity [10]. This is a tri-axial orthogonal constraint, where values measured on each axis are not independent. For a tri-axial gyroscopic system, property (p2): the gravity vector measured using a static tri-axial accelerometer must equal the gravity vector computed using the IMU orientation integration algorithm, which in turn uses the angular velocities measured using the gyroscopes [11].

For accelerometer, let a_0 be the acceleration vector measured by the accelerometer and a is the actual input acceleration provided to the accelerometer, governed by the "Eq. 1".

$$a = MS(a_o - b_a) \qquad (1)$$

$$a=\begin{bmatrix}a_x\\a_y\\a_z\end{bmatrix},\ a_o=\begin{bmatrix}a_{ox}\\a_{oy}\\a_{oz}\end{bmatrix},\ S=\begin{bmatrix}S_{xx}&0&0\\0&S_{yy}&0\\0&0&S_{zz}\end{bmatrix},\ M=\begin{bmatrix}1&-\alpha_{yz}&\alpha_{zy}\\\alpha_{xz}&1&-\alpha_{zx}\\-\alpha_{xy}&\alpha_{yx}&1\end{bmatrix},\ b_a=\begin{bmatrix}b_{ax}\\b_{ay}\\b_{az}\end{bmatrix} \quad (2)$$

Where, b is the bias vector, M is axis misalignment axis matrix and S the scale factor matrix. M is the axis misalignment correction matrix each α_{ij} represents the small angle deviation of the i^{th} sensitivity axis of the accelerometer around the j^{th} sensitivity axis of the IMU [9], as indicated in "**Fig. 1**". The misalignment error is usually small for the tri-axis MEMS sensors, but the misalignment between different tri-axial sensors can be large.

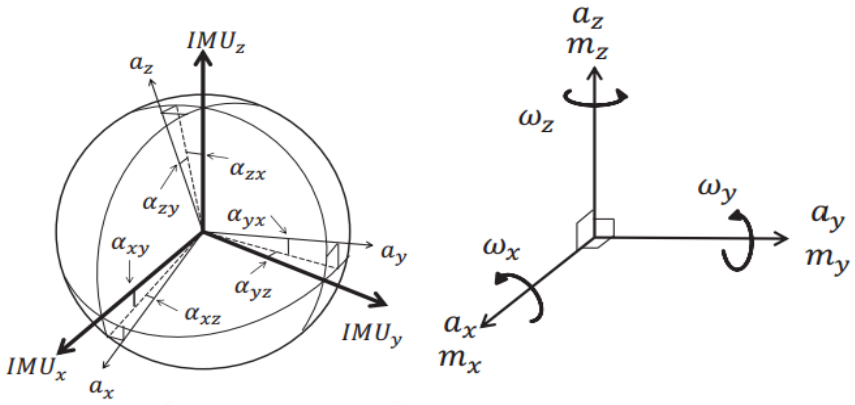

Figure 1 Misalignment between Axes and Axes of Sensors Alignment (Ideal)

The calibration for the accelerometer aims to find the best fitted parameters in the constant matrices S, M and the constant vector b_a which constitute the least error in the acceleration measurement. Since the constant matrices S, M will be multiplied together as given in "Eq. 3".

$$\Theta_a=\begin{pmatrix}e_{00}&e_{01}&e_{02}\\e_{10}&e_{11}&e_{12}\\e_{20}&e_{21}&e_{22}\end{pmatrix} \quad (3)$$

Where Θa is a constant and diagonally dominant matrix, therefore the numbers of parameters being solved are reduced to twelve in total including nine elements in Θa and three elements in b_a.

The cost function, as proposed in [9], is utilizing the fact that the magnitude of gravity vector is 1g. Therefore the cost is equal to the sum of squared errors of the N sets of static measurements from 1g such that the 12 parameters are optimized by "Eq. 4".

$$(\Theta_a, b_a)=\arg\min_{\Theta_a,b_a}\sum_{n=1}^{N}(1-\|a\|_2)^2 \quad (4)$$

Similar to the accelerometer error model, the calibration of the gyroscope also includes the diagonal scaling matrix S, the axis mis-alignment matrix M, the bias vector b_g. The gyroscope error model is given by "Eq. 5".

$$g=MS(g_o-b_g) \quad (5)$$

Where, g is the corrected angular rates and g_0 is the raw measurement vector with respect to the sensor axes. And this error model can also be simplified one step further to 12 calibration parameters including Θg and b_g. Where Θg is the resultant matrix multiplied by the mis-alignment matrix, the scaling matrix and the rotation matrix that aligns the gyroscope sensor frame on the calibrated accelerometer frame.

Being different from the cases of accelerometer calibration, since there is no accurate platform measuring precise angular velocities, direct comparisons between ideal and noisy angular rates no longer applies. The cost function [8] for the gyroscope calibration provides a suitable means to optimize the gyroscope parameters, which basically calculates the resultant orientation change between two static intervals by integrating the measured angular rates, then applies the resultant rotation to the prior static calibrated gravity vector to yield the new gravity vector. By adopting the fact that ideally the rotation by angular rates integration should result in the same orientation change reflected by the differences between the prior and posterior gravity vector, the errors between the gravity vector in the posterior static interval and the new gravity vector serves as the cost function for calibrating the rate gyroscope.

The rotation matrix R is obtained from gyroscope readings and is used for computing the new gravity v_a vector from the prior calibrated gravity vector u_a as given by "Eq. 6".

$$v_a=R(u_a) \quad (6)$$

Now the cost function for calibrating the rate gyroscope is modified such that the parameters to be optimized are given in "Eq. 7".

$$(\Theta_g, b_g)=\arg\min_{\Theta_g,b_g}\sum_{n=1}^{N}(\|v_a-u_a^{'}\|_2)^2 \quad (7)$$

Where, u'_a is the calibrated gravity vector in the posterior static interval by the accelerometer. The above optimization for the gyroscope is valid for arbitrary motions between two static intervals. The calibrated vectors u_a, u'_a are calculated by applying the optimized parameter sets after the accelerometer calibration to their raw measurements.

III. ALLAN VARIANCE

Allan variance is a method of representing RMS random drift error as a function of average time. It is simple to compute and relatively simple to interpret and understand. Allan variance method is used to characterize various types of noise terms in the inertial sensor data by performing certain operations on the entire length of data [11]. By performing these simple operations, a characteristic curve is obtained whose inspection provides systematic characterization of various random errors present in the inertial sensor output data.

Allan variance is based on the method of cluster analysis. A data stream is divided into clusters of specified length. Assume there are *N* consecutive data points, each having a sample time of t_0. Forming a group of *n* consecutive data points (with $n<N/2$), each member of the group is a cluster, as shown in "**Fig. 2**".

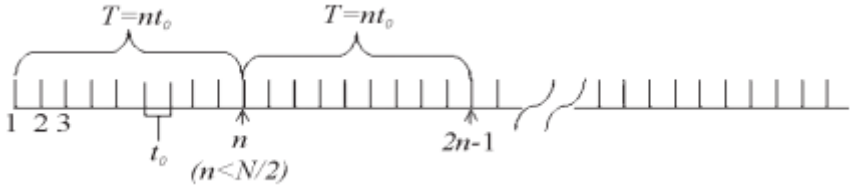

Figure 2 Schematic of the data structure used in the derivation of allan variance.

Associated with each cluster is a time, T, which is equal to nt0. If the instantaneous output rate of inertial sensor is Ω(t) the cluster average is defined by 'Eq. 8'.

$$\Omega_k(T) = \frac{1}{T}\int_{t_k}^{t_k+T} \Omega(t)dt \qquad (8)$$

where Ωk(T) represents the cluster average of the output rate for a cluster which starts from the kth data point and contains n data points. The definition of the subsequent cluster average is given by 'Eq. 9'.

$$\Omega_{next}(T) = \frac{1}{T}\int_{t_{k+1}}^{t_{k+1}+T} \Omega(t)dt \qquad (9)$$

where tk+1 = tk +T. Performing the average operation for each two adjoining clusters and form the differences as given in 'Eq. 10'.

$$\xi_{k+1,k} = \Omega_{next}(T) - \Omega_k(T) \qquad (10)$$

For each cluster time *T*, the ensemble of ξ defined by 'Eq. 10' forms a set of random variables. The quantity of interest is the variance of ξs over all the clusters of the same size that can be formed from entire data [12]. Thus, the Allan variance of length T is defined by 'Eq 11'.

$$\sigma^2(T) = \frac{1}{2}\left\langle \left[\Omega_{next}(T) - \Omega_k(T)\right]^2 \right\rangle \qquad (11)$$

The brackets<> in 'Eq. 11' denote the averaging operation over the ensemble of clusters. Thus, above equation can be rewritten as in 'Eq. 12'.

$$\sigma^2(T) = \frac{1}{2(N-2n)}\sum_{k=1}^{N-2n}\left[\Omega_{next}(T) - \Omega_k(T)\right]^2 \qquad (12)$$

Clearly, for any finite number of data points (*N*), a finite number of clusters of a fixed length (*T*) can be formed. Hence, 'Eq. 12' represents an estimation of the quantity $\sigma^2(T)$,whose quality of estimate depends on the number of independent clusters of a fixed length that can be formed. The Allan variance is a measure of the stability of sensor output. The Allan variance method provides a means of identifying and quantifying various noise terms that exist in the data. It is normally plotted as the square root of the Allan variance versus *T*, [$\sigma(T)$], on a log log plot and various noise coefficients are calculated from the plot.

The cluster sampling can be done in following three ways that is [13] (a) Fully Overlapping Allan Variance (b) Non Overlap Allan Variance (c) Not Fully Overlapping Allan Variance as shown in "**Fig. 3**".

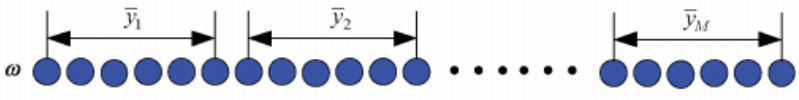

(a) Non overlapped clustering

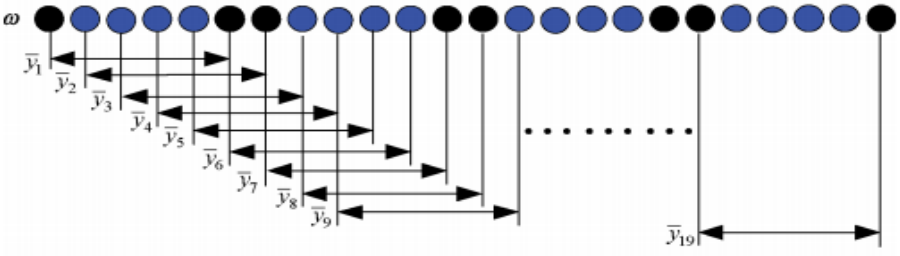

(b) Fully overlapping clustering

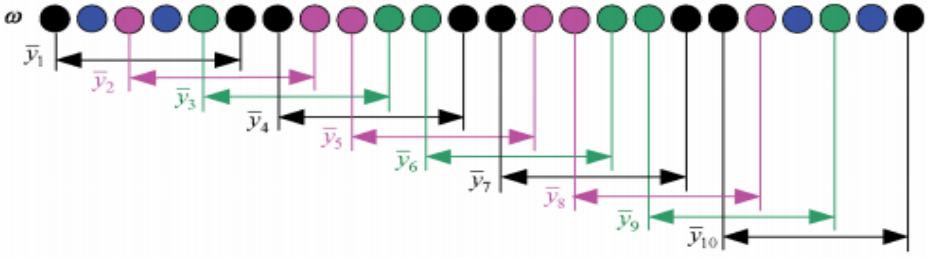

(c) Non fully overlapping clustering

Figure 3 Cluster sampling methods (a) Non overlapped cluster sampling method (b) Fully overlapping cluster sampling method (c) Not fully overlapping cluster sampling method

Noise terms in allan variance are represented as given below [11]:

a) Quantisation noise: Allan variance for quantisation noise is given by 'Eq. 13'.

$$\sigma^2(T) = \frac{3Q_Z^2}{T^2} \qquad (13)$$

Where, *Qz* is the quantisation noise coefficient and *T* is the sample interval. Therefore the root Allan variance of the quantisation noise when plotted in a log-log scale is represented by a slope of -1.

b) Angle (velocity) random walk: High frequency noise terms, that have correlation time, much shorter than the sample time can contribute to the gyro angle (or accelerometer velocity) random walk. The Allan variance for angle (velocity) random walk is given by 'Eq. 14'.

$$\sigma^2(T) = \frac{N^2}{T} \qquad (14)$$

Equation 14 indicates that a log-log plot of σ^2 (T) versus T has a slope of -1/2.

c) Bias instability: The origin of this noise is the electronics, or other components susceptible to random flickering. Because of its low-frequency nature, it shows as the bias fluctuations in the data. Allan variance for bias instabilityis given by 'Eq. 15'.

$$\sigma^2(T) = \left(\frac{B}{0.6648}\right)^2 \qquad (15)$$

Hence, the bias instability value can be read off the root Allan variance plot at the region where the slope is zero.

d) Rate random walk: This noise is a result of integrating wideband acceleration PSD. This is a random process of uncertain origin, possibly a limiting case of an exponentially correlated noise with a very long correlation time. The Allan variance of rate random walk is given by 'Eq. 16'.

$$\sigma^2(T) = \frac{K^2 T}{3} \qquad (16)$$

This indicates that rate random walk is represented by a slope of + 1/2 on a log-log plot of $\sigma(T)$ versus T.

e) Rate ramp: This is more of a deterministic error rather than a random noise. It could also be due to a very small acceleration of the platform in the same direction and persisting over a long period of time. Allan variance of rate ramp is given by 'Eq. 17'.

$$\sigma^2(T) = \frac{R^2 T^2}{2} \qquad (17)$$

This indicates that the rate ramp noise has slope of + 1 in the log-log plot of $\sigma(T)$ versus T.

Sample plot of allan variance is shown in "**Fig. 4**".

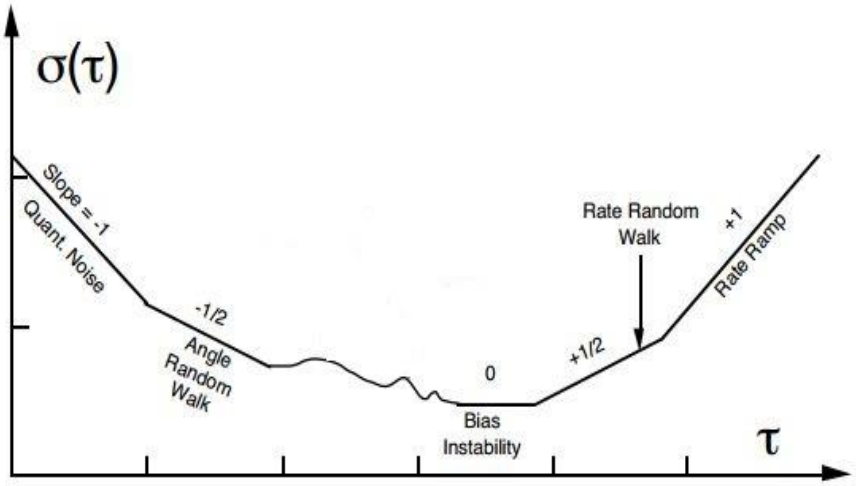

Figure III $\sigma(T)$ Sample plot of Allan variance analysis results

IV. EXPERIMENTAL SETUP AND RESULTS

Xsens MTi-G700 IMU was used for evaluating the use of In Field Calibration and Allan Variance for sensor error parameter determination. Tests were carried out at room temperature. The Xsens MTi-G-700 is a solid state inertial sensing system used for measuring linear accelerations and angular rates. Xsens MTi-G700 is connected with computer through a USB cable. MT Software Suit is used for data acquisition for MTi-G-700. The inertial sensor output data are decoded at 100 Hz data rate. The output of gyro data is delta angle with units in ^{0}/s and that of accelerometer is the delta acceleration with units in m/s^2.

The mathematical calculation model is developed for In Field Calibration and Allan Variance under the MATLAB environment according to the methodology discussed in chapter four and five. Three-axis sensor data can be loaded at the same time. In addition, the input parameters include the number of total data points and sample rate. Then the MATLAB will output the calibration parameters and allan variance result plot with identified noise coefficients.

Calibration Results: For the tri-axial accelerometer, the IMU is placed in 18positions, i.e., N=18, to obtain 18 readings to compute the cost function (Θa, ba). These 18 positions consist of resting the IMU on its six flat faces and 12 edges. This proposed arrangement allows gravity vector measurements to be spread evenly over the unit sphere about the center of the platform frame. As there are 12 model parameters to fit, it is prudent to have more than that number of measurements. Next, the static signals are averaged over a period of 1 s to reduce noise. (Θa, ba) is minimized using the optimization tool available in MATLAB environment. The initial parameter values are set using the nominal values.

After the accelerometer has been calibrated, it can be used to serve as a static gravity vector sensor for calibrating the gyroscopes. Eighteen sets of continuous accelerometer and gyroscope samples are taken. After the accelerometer has been calibrated, it can be used to serve as a static gravity vector sensor for calibrating the gyroscopes. Eighteen sets of continuous accelerometer and gyroscope samples are taken. The process of computing the gyroscope error model parameter values uses the same nonlinear optimization method as in the case of the accelerometers. Computed model parameters for accelerometer and gyroscope are shown in "**Table I**".

Table I Model Prameters for accelerometer and gyroscope

Model Parameters	Accelerometer	Gyroscope
e_{00}	131.08	3107.21
e_{01}	0.008432	0.0001369
e_{02}	0.003694	-0.02182
e_{10}	-0.008030	0.009694
e_{11}	131.579	3145.92
e_{12}	0.003694	-0.0078
e_{20}	0.02513	-0.003377
e_{21}	-0.01386	-0.01095
e_{22}	131.766	3107.85
b_x	32787	32524.5
b_y	32772.4	32768.2
Bz	32757.2	32974.1

In the table e_{00},e_{11}, e_{22}represents scale factor while e_{01}, e_{02}, e_{10},e_{12},e_{20},e_{21} represents non-orthogonalities and b_x, b_y, b_z represents the respective bias of accelerometer and gyroscope.

Allan Variance Results: The IMU is fixed on the platform and placed in a room with uniform temperature. The raw data were collected for 2 *h* with sample rate of 100 *Hz*. The raw data are the counts of the pulse output of gyroscopes and accelerometers, and are converted by using their scale factor to the unit of *deg/h* and *m/s*^{2}, respectively.

In order to investigate the performance of the variance analysis methods stated in chapter four, we choose a dataset of 600 *s*. This dataset contains 60000 data points. The log–log plots of the three basic Allan deviation results versus cluster time are presented below:

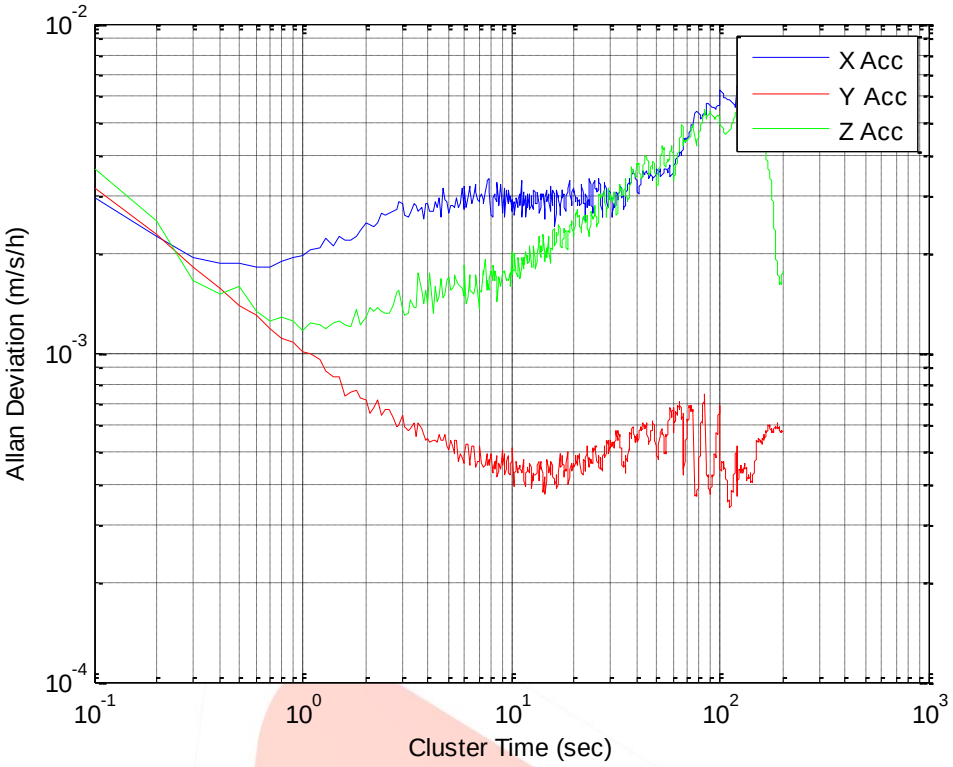

Figure IV Non-overlapped Allan Deviation plot for X, Y and Z accelerometer

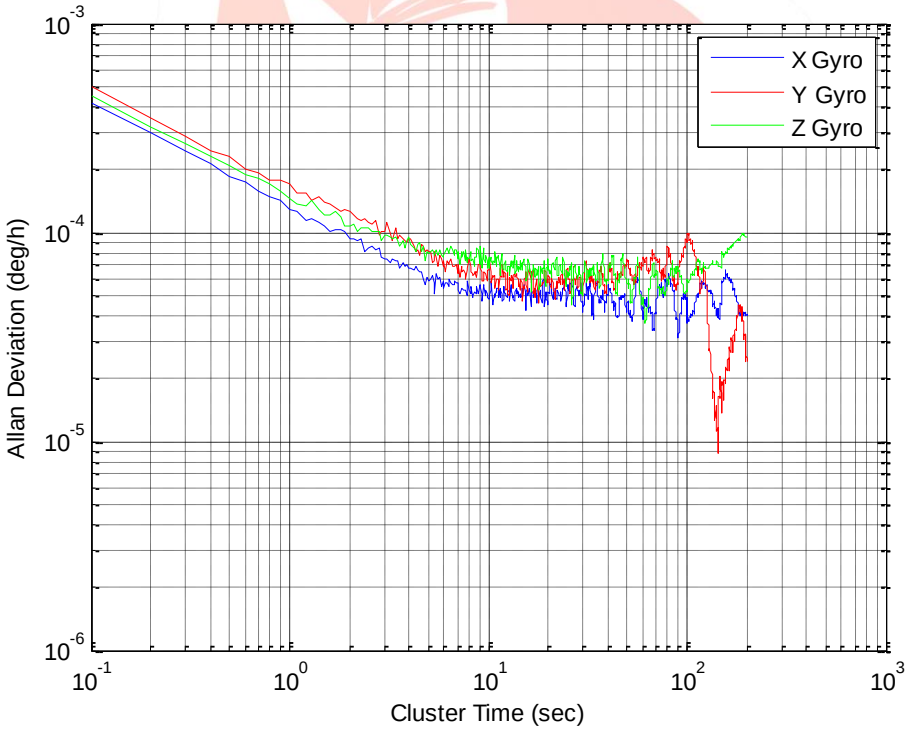

Figure 6 Non-overlapped Allan Deviation plot for X, Y and Z gyroscope

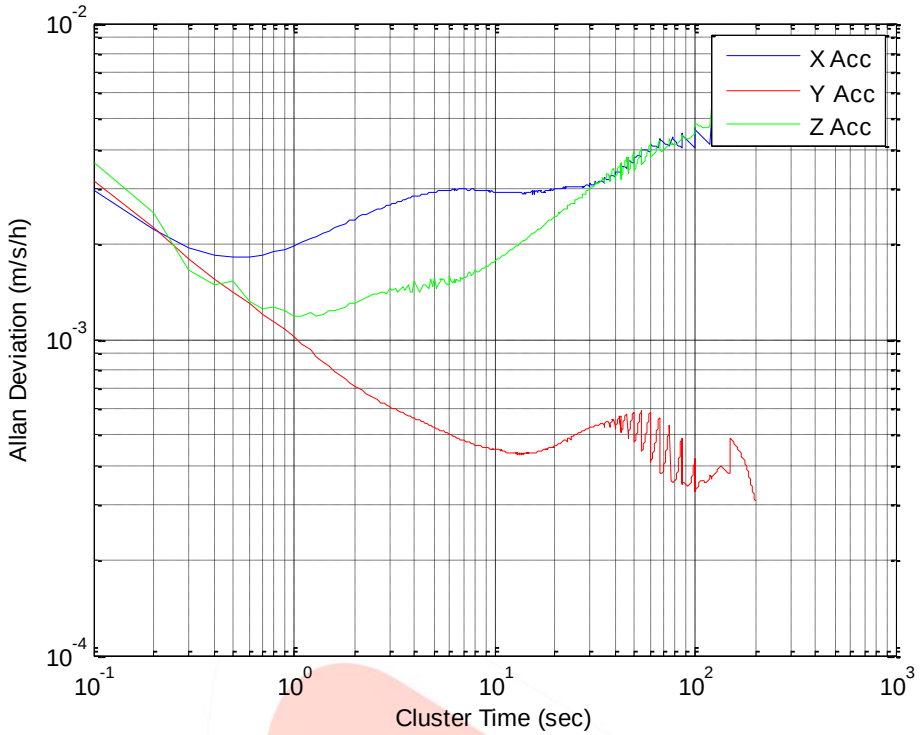

Figure 7 Not fully overlapped Allan Deviation plot for X, Y and Z accelerometer

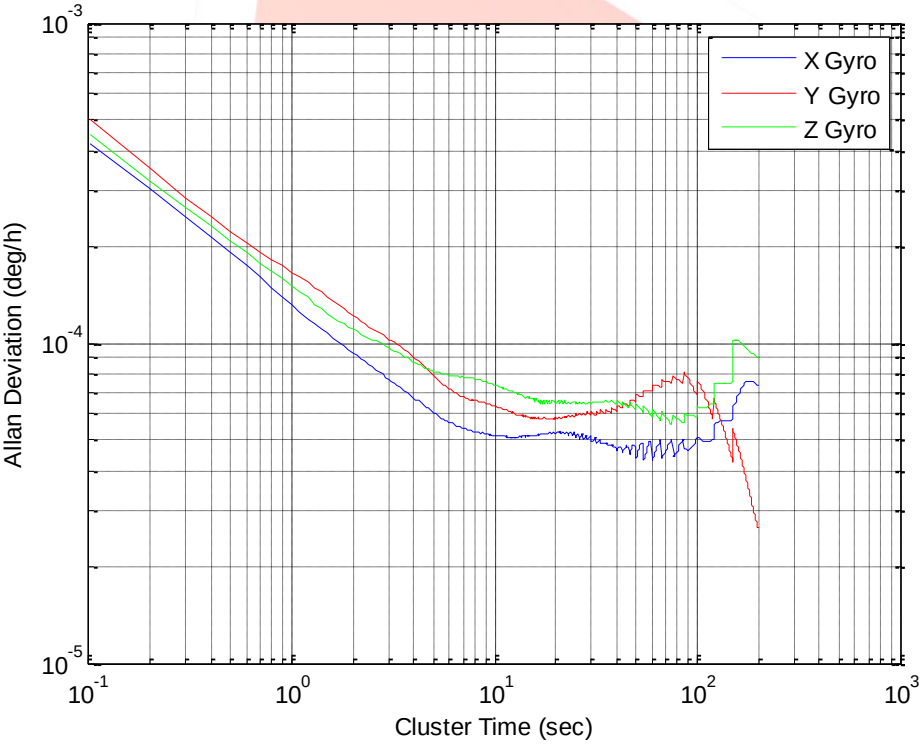

Figure 8 Not fully overlapped Allan Deviation plot for X, Y and Z gyroscope

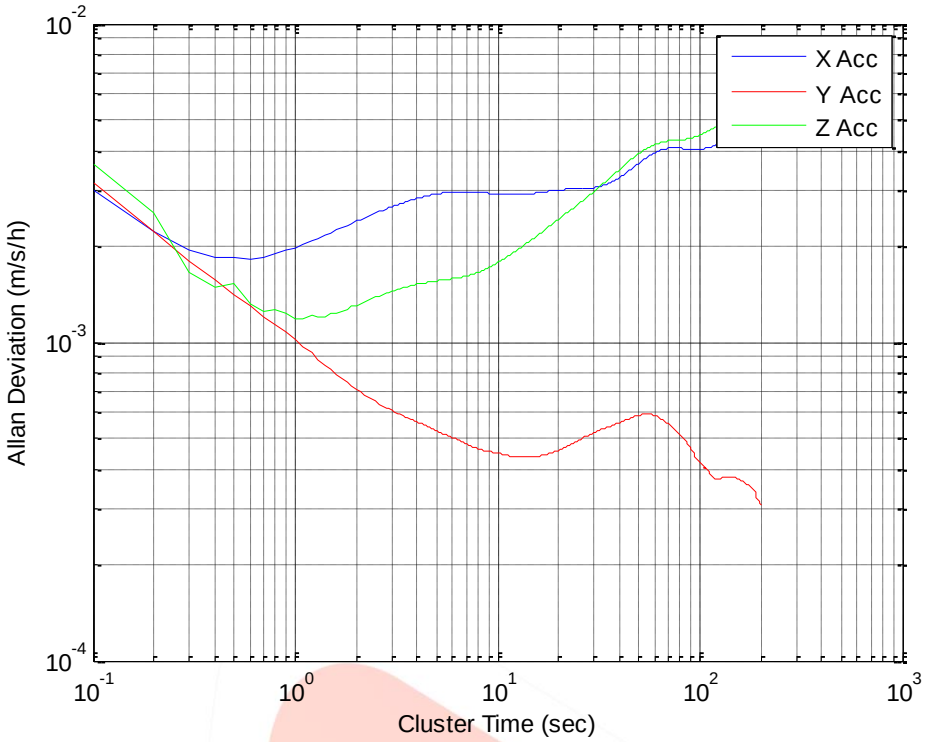

Figure 9 Fully overlapped Allan Deviation plot for X, Y and Z accelerometer

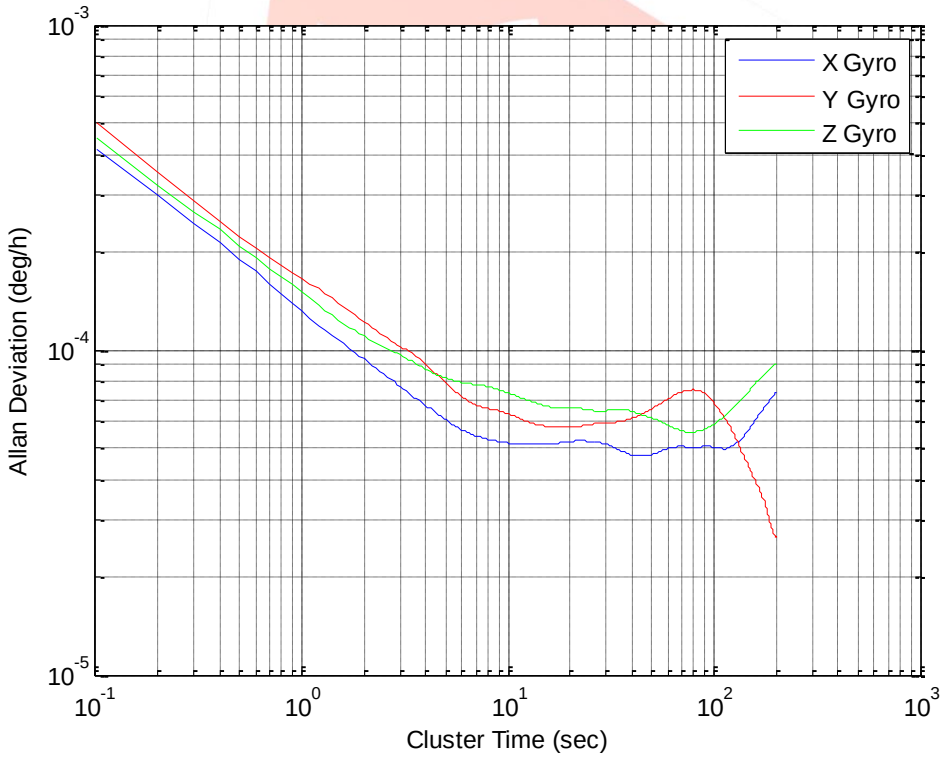

Figure 10 Fully overlapped Allan Deviation plot for X, Y and Z gyroscope

From above figures it is clear that the curves of non-fully overlap and fully overlap allan deviation are very smooth, whereas the curve of non-overlap allan deviation shows greater variation. The standard deviations indicate that, for short cluster time, the non-overlap allan deviation, non-fully overlap allan deviation and fully overlap allan deviation are good enough with each other; whereas for middle and long cluster time, the non-fully overlap allan deviation and fully overlap allan deviation are much better than non-overlap allan deviation, and the non-fully overlap allan deviation is almost the same as fully overlap allan deviation, but the calculation time of non-fully overlap allan deviation is much less than fully overlap allan deviation.

The identified noise coefficients from Allan Deviation plot for accelerometer and gyroscope x, y and z axis are given by "**Table II**" and "**Table III**".

Table II Identified error coefficients for accelerometer x, y and z axis

Accelerometer	**x axis**	**y axis**	**z axis**

Quantization Noise	N/A	N/A	$8x10^{-8}$
Angle Random Walk	$1.6x10^{-5}$	$1.7x10^{-5}$	$1.9x10^{-5}$
Bias Instability	$1.8x10^{-3}$	$4.3x10^{-4}$	$1.2x10^{-3}$
Rate Random Walk	N/A	N/A	$5x10^{-2}$
Rate Ramp	N/A	N/A	N/A

Table III Identified error coefficients for gyroscope x, y and z axis

Gyroscope	**x axis**	**y axis**	**z axis**
Quantization Noise	N/A	N/A	N/A
Angle Random Walk	$2.3x10^{-6}$	$3x10^{-6}$	$2.5x10^{-6}$
Bias Instability	$4.7x10^{-5}$	$5.7x10^{-5}$	$5.5x10^{-5}$
Rate Random Walk	N/A	$9x10^{-4}$	$6x10^{-4}$
Rate Ramp	$2x10^{-3}$	N/A	N/A

The Allan variance method presented has proven to be able to identify the characterization of various random errors contained in the output data of inertial sensors. By performing a simple operation on the entire length of data, a characteristic curve is obtained whose inspection facilitates the determination of the different types and magnitude of noise terms existing in inertial sensors.

V. CONCLUSION

Calibrating and Modeling inertial sensors are the first and the most difficult step in the INS designs. This technical report summarizes the major deterministic and stochastic error models of low cost inertial sensors. Inertial sensors are basically composed of two types of errors i.e deterministic and random errors. Deterministic errors can be eliminated by calibration methods whereas random errors can be compensated by stochastic modeling techniques. Various calibration methods were studied in order to calibrate the inertial sensors. Some calibration methods require high precision rate table for calibration and also there are few calibration techniques which does not require such high end instruments. In this thesis calibration was done using in field calibration which does not require any high precision rate table. For stochastic modeling of sensors, allan variance technique was used.

VI. AKNOWLEDGMENT

This study was supported in part by research fund from the CSIR-Central Scientific Instruments Organisation, Chandigarh, India.

REFERENCES

[1] J. K. Bekkeng, "Calibration of a novel MEMS inertial reference unit," Instrumentation and Measurement, IEEE Transactions on, vol. 58, pp. 1967-1974, 2009.
[2] P. Aggarwal, Z. Syed, X. Niu, and N. El-Sheimy, "A standard testing and calibration procedure for low cost MEMS inertial sensors and units," Journal of navigation, vol. 61, pp. 323-336, 2008.
[3] Nassar, S, "Improving the Inertial Navigation System (INS) Error Model for INS and INS/DGPS Applications," PhD Thesis, Department of Geomatics Engineering , University of Calgary, Canada, UCGE Report No. 20183, 2003.
[4] Priyanka Aggarwal, Zainab Syed, Aboelmagd Noureldin, Naser El-Sheimy, "MEMSBased Integrated Navigation," GNSS Technology and Application Series, ISBN-13:978-1-60807-043-5, 2010.
[5] Hou, H., and El-Sheimy, N., "Inertial Sensors Errors Modeling Using Allan Variance" Proceedings of ION GNSS 2003, Portland, Oregon, Sept. 9–12, 2003.
[6] El-Sheimy N, Inertial Techniques and INS/DGPS Integration: Lecture Notes ENGO 623. Dept. of Geomatics Eng., University of Calgary, Calgary, Canada, 2003.
[7] IEEE Std 1293, "IEEE Standard Specification Format Guide and Test Procedure for Linear, Single-Axis, Non-gyroscopic Accelerometers", 1998.
[8] Fong, W. T., S. K. Ong, And A. Y. C. Nee., "Methods for In-Field User Calibration of an Inertial Measurement Unit without External Equipment", Measurement Science and Technology 19, No. 8 (2008): 085202, 2008.
[9] I. Skog and P. Handel, "Calibration of a MEMS inertial measurement unit," in XVII IMEKO World Congress, 2006.
[10] Cheuk, Chi Ming, Tak Kit Lau, Kai Wun Lin, and Yunhui Liu, "Automatic calibration for inertial measurement unit", In Control Automation Robotics & Vision (ICARCV), 2012 12th International Conference on, pp. 1341-1346. IEEE, 2012.
[11] R. Ramalingam, G. Anitha and J. Shanmugam, "Microelectromechnical Systems Inertial Measurement Unit Error Modelling and Error Analysis for Low-cost Strapdown Inertial Navigation System", Defence Science Journal, Vol. 59, No. 6, DESIDOC, pp. 650-658, November 2009.
[12] IEEE Std 952, "IEEE Standard Specification Format Guide and Test Procedure for Single-Axis Interferometric Fiber Optic Gyros", 1997.
[13] Jintao Li and Jiancheng Fang, "Not Fully Overlapping Allan Variance and Total Variance for Inertial Sensor Stochastic Error Analysis", IEEE Transactions On Instrumentation And Measurement, 0018-9456, IEEE 2013.